Concurrent Changes in *Dunaliella salina* Ultrastructure and Membrane Phospholipid Metabolism after Hyperosmotic Shock

Kregg J. Einspahr, Manabu Maeda, and Guy A. Thompson, Jr.

Department of Botany and Division of Biological Sciences, University of Texas, Austin, Texas 78713

Abstract. Hyperosmotic shock, induced by raising the NaCl concentration of *Dunaliella salina* medium from 1.71 to 3.42 M, elicited a rapid decrease of nearly one-third in whole cell volume and in the volume of intracellular organelles. The decrease in cell volume was accompanied by plasmalemma infolding without overall loss of surface area. This contrasts with the dramatic increase in plasmalemma surface area after hypoosmotic shock (Maeda, M., and G. A. Thompson. 1986. *J. Cell Biol.* 102:289–297). Although plasmalemma surface area remained constant after hyperosmotic shock, the nucleus, chloroplast, and mitochondria lost membrane surface area, apparently through membrane fusion with the endoplasmic reticulum. Thus the endoplasmic reticulum serves as a reservoir for excess membrane during hyperosmotic stress, reversing its role as membrane donor to the same organelles during hypoosmotically induced cell expansion. Hyperosmotic shock also induced rapid changes in phospholipid metabolism. The mass of phosphatidic acid dropped to 56% of control and that of phosphatidylinositol 4,5-bisphosphate rose to 130% of control within 4 min. Further analysis demonstrated that within 10 min after hyperosmotic shock, there was 2.5-fold increase in phosphatidylcholine turnover, a twofold increase in lysophosphatidylcholine mass, a four-fold increase in lysophosphatidate mass, and an elevation in free fatty acids to 124% of control, all observations suggesting activation of phospholipase A. The observed biophysical and biochemical phenomena are likely to be causally interrelated in providing mechanisms for successful accommodation to such severe osmotic extremes.

MECHANISMS by which eukaryotic cells tolerate acute and chronic osmotic stress are not well understood. The unicellular alga *Dunaliella salina* possesses extremely effective mechanisms for tolerating such osmotic stress. It will grow in saline environments ranging from 0.5 to 5 M NaCl and successfully accommodates rapid and drastic changes in extracellular osmolarity (Brown and Borowitzka, 1979).

Previously, we have demonstrated that the response of *D. salina* to hypoosmotic shock involves rapid alterations in membrane morphology (Maeda and Thompson, 1986) and equally rapid changes in phospholipid metabolism (Einspahr et al., 1988). The increase in cell volume that follows rapid transfer (2–4 s) to hypotonic medium is accommodated by increased plasmalemmal surface area through rapid vesicle fusion. More recently, we have reported that the response of *D. salina* to hypoosmotic shock also involves the rapid breakdown of the polyphosphoinositides, phosphatidylinositol 4,5-bisphosphate (PIP_2),[1] and phosphatidylinositol 4-monophosphate (PIP) through the apparent activation of a specific phospholipase C (Einspahr et al., 1988). The rapid breakdown of the polyphosphoinositides after hypoosmotic shock is accompanied by a sharp increase in the levels of phosphatidic acid (PA), leading us to propose the activation of an inositol phospholipid signal transduction pathway as described in a variety of cell systems responding to other types of stimuli (Sekar and Hokin, 1986).

The purpose of the present investigation was to (*a*) analyze the changes in membrane organization and phospholipid metabolism in *D. salina* after hyperosmotic shock, (*b*) identify specific factors among these changes which are likely to be important in accommodation to hyperosmotic shock, and (*c*) compare and contrast such changes with those incurred by *D. salina* after hypoosmotic shock.

Our results indicate that the changes in membrane disposition and phospholipid metabolism induced by hyperosmotic shock are fundamentally different than those induced by hypoosmotic shock. Furthermore, these changes appear to be significant factors in the spatial reorganization of *D. salina* after hyperosmotic shock. They may also provide im-

Manabu Maeda's present address is Department of Dermatology, Gifu University School of Medicine, Tsukasamachi 40, Gifu, Japan.

1. *Abbreviations used in this paper*: Ch, chloroplast; ER, endoplasmic reticulum; Gol, Golgi bodies; IMP, intramembranous particles; lysoPA, lysophosphatidic acid; lysoPC, lysophosphatidylcholine; Mt, mitochondria; N, nucleus; OE, outer membrane of the chloroplast envelope; PA, phosphatidic acid; PC, phosphatidylcholine; PE, phosphatidylethanolamine; PG, phosphatidylglycerol; PI, phosphatidylinositol; PIP, phosphatidylinositol 4-monophosphate; PIP_2, phosphatidylinositol 4,5-bisphosphate; PM, plasma membrane; TLC, thin layer chromatography; V, vesicle; Va, vacuole.

portant physiological cues for metabolic alterations that allow successful accommodation to such severe osmotic stress.

Materials and Methods

Cell Culture

Cultures of *D. salina* (UTEX 1644) were grown under continuous light (100 $\mu E \times m^{-2} \times s^{-1}$) in 1-liter Erlenmeyer flasks containing 500 ml of synthetic medium bubbled with 0.5% CO_2-enriched air at 30°C (Lynch and Thompson, 1982). Under these conditions, the cells grew with a generation time of 20 h. Cultures used for experiments were grown to the mid-logarithmic stage (0.5–1.0 × 10^6 cells/ml).

Chemicals

Carrier free [^{32}P]-orthophosphate in water was purchased from DuPont-New England Nuclear, Boston, MA. Phosphatidylinositol (PI) (soybean), PIP (bovine brain), PIP_2 (bovine brain), PA (egg yolk), lysophosphatidylinositol (soybean), lysophosphatidic acid (lysoPA) (oleoyl, synthetic), lysophosphatidylcholine (lysoPC) (soybean), lysophosphatidylethanolamine (palmitic, synthetic), and lysophosphatidylglycerol were purchased from Sigma Chemical Co., St. Louis, Mo.

Light Microscopy

Cell shape and length alterations due to hyperosmotic stress were observed by light microscopy beginning within 10 s after raising the NaCl concentration to 3.42 M. These experiments were performed three times using logarithmic phase cells. More than 10 micrographs (×4,000) were made 3 ± 1 min after the culture medium was raised to 3.42 M NaCl by the rapid addition (5 s) of 5.12 M NaCl synthetic medium with continuous mixing.

Electron Microscopy

Samples used for freeze-fracture analysis were fixed for 2–3 h at 30°C under illumination with 2–2.5% glutaraldehyde buffered with the synthetic medium for *D. salina* as described by Lynch and Thompson (1982). Samples were washed three times with synthetic medium and then transferred through increasing concentrations of glycerol, terminating with 30% glycerol buffered with the synthetic medium. The cells were pelleted in a clinical centrifuge at 1,500 *g* for 5 min and kept frozen in Freon until they were fractured in a Balzers BF 400 device. In some cases, living cells were rapidly quenched in Freon without fixation and cryoprotectant treatment. Replication was performed with platinum-carbon, and the replicas were coated with carbon. After residual tissue was digested from the replicas with sodium hypochlorite (Clorox), they were given three rinses in water before collection on 300 or 400 mesh grids. Electron microscopy was performed on a Hitachi-11E electron microscope operating at 50 kV. Intramembranous particles (IMP) were counted in 20–30 randomly selected areas (0.2 × 0.2 μm^2) of several different micrographs enlarged 48,000 times and were expressed as particles per micrometer squared.

Samples to be used for preparing thin sections were fixed in 2–2.5% glutaraldehyde by the same method as just described. After being rinsed three times in synthetic medium, samples were postfixed in 1% (wt/vol) OsO_4 for 1 h, transferred to 25% acetone for 30 min, and then to increasing concentrations of acetone, terminating with 100% acetone for dehydration. Finally, they were embedded in Spurr's low viscosity medium (Spurr, 1969). Sections cut on a MT-1 microtome were collected on 400 mesh grids, stained in uranyl acetate for 3 min and then in lead citrate for 3 min. Micrographs were made using a Hitachi-11E electron microscope at an accelerating voltage of 50 kV.

Cell Volume and Surface Area of Plasma Membrane

Cell volume was calculated from light microscopy data by using the equation for prolate ellipsoids ($V = 4/3\ \pi\ ab^2$, where $a \geqslant b$), although hyperosmotically stressed cells appeared more like irregular cucumber-shaped ellipsoids by thin-section electron microscopy. Surface areas of both control and stressed cells were determined from thin-section electron micrographs using the formula:

$$\frac{S}{V} = \frac{2I_L}{P_P}$$

Table I. Changes in Cell Volume and Cell Surface Area Caused by Hyperosmotic Shock

	Control culture	Stressed culture	Vol stressed / Vol control
n	57	48	–
$\bar{a}$ (μm)	6.05 ± 0.74	7.25 ± 0.65	1.20
$\bar{b}$ (μm)	4.79 ± 0.47	3.62 ± 0.41	0.76
Volume (μm^3)	591 ± 161	398 ± 178	0.67
Surface area* (μm^2)	350	349	–

Living cells were photographed 3 ± 1 min after the NaCl concentration was raised from 1.71 to 3.42 M. n, number of cells counted. $\bar{a}$, average ± SD of half-long diameter. $\bar{b}$, average ± SD of half-short diameter.
* Actual surface area was obtained by morphometric analysis of electron micrographs (see Materials and Methods).

where S = surface area, V = volume, I_L = number of intersections per unit test line (regular lattice grid, distance between points [d] of 8 mm was used on ×4,600 micrographs), and P_P = point density or point fraction (Weibel, 1979; Toth, 1982).

General Morphometric Analysis: Stereology

Many thin section micrographs were utilized for morphometric analysis following techniques described by Weibel (1979). Regular lattice grid points (d = 25 mm) were counted on the micrographs (×48,000) of control and stressed cells for obtaining volumes of vacuoles (Va), chloroplasts (Ch), nuclei (N), mitochondria (Mt), and Golgi bodies (Gol).

Estimations of endoplasmic reticulum (ER) and Gol surface area were achieved by counting their intersections with a curvilinear grid (Merz pattern; d, 30 mm) on the micrographs (×48,000) of control and stressed cells. The average surface area of specific organelles per meter cubed of cell volume (S_v) was calculated from the formula $S_v = 2I_t/k \cdot d' \cdot P_t$, where k = 2 (lattice grid) or 1.57 (Merz pattern), d' = d corrected to actual magnification, P_t = total number of grid points within the internal cell area, and I_t = the total intersections with the lattice grid. Then the total surface area per cell (S_t) was calculated from S_v and the actual cell volume (see Table I). Estimations of actual surface area of Ch, Mt, N, Va, and vesicles (V) were made by counting intersection numbers (I_t) with a lattice grid (d, 25 mm) on a minimum of 19 separate micrographs (×48,000).

Lipid Analyses

Lipids were extracted as described previously in detail (Einspahr et al., 1988). Briefly, lipids were extracted from cells with ice-cold chloroform/methanol/conc. HCl (200/100/1.5, vol/vol/vol). The organic phase containing extracted lipid was washed once with 0.6 vol of chloroform/methanol/1 M HCl (3/45/45, vol/vol/vol), and once with 0.6 vol of chloroform/methanol/0.01 M HCl (3/45/45, vol/vol/vol) and then concentrated to dryness under N_2 and redissolved in chloroform/methanol (2/1, vol/vol).

Phospholipids were separated by thin layer chromatography (TLC) using silica gel H (EM Science, Cherry Hill, NJ) containing 2.5% (dry weight) of potassium oxalate. The solvent system (system A) routinely used to separate the major phospholipids as well as the quantitatively minor inositol phospholipids and lysoPC was chloroform/acetone/methanol/acetic acid/H_2O (40/15/13/12/8, by vol) (Jolles et al., 1979). Verification of lysoPC identification and quantification in addition to analyses of other lysophospholipids was accomplished in the solvent system (system B) chloroform/methanol/4.2 N NH_4OH (90/70/20, vol/vol/vol) and a two-dimensional solvent system employing system B in the first dimension followed by 20 min of drying under a partial vacuum in a vacuum oven (National Appliance Co., Portland, OR) and development in system A in the second dimension. Phospholipid bands were visualized by briefly exposing the plate to iodine vapor. Neutral lipid classes were separated by TLC on silica gel H plates (containing no potassium oxalate) using the solvent system petroleum ether/ethyl ether/acetic acid (70/30/1, vol/vol/vol). After drying the plate under N_2 a glass plate was placed over lanes containing the separated sample and lipids in a reference lane were visualized by brief exposure to I_2 vapors.

The minor inositol phospholipids, PA, and lysophospholipids were detected with the aid of standards spotted on TLC plates with the extract or in adjacent lanes. Radioactivity of individual lipid bands was determined

as described previously (Einspahr et al., 1988). Phosphorus content of lipid extracts was quantified by the method of Bartlett (1959) as modified by Marinetti (1962). The phosphorus content of individual phospholipid bands separated by TLC was quantified by the method of Rouser et al., (1970). Analysis of free fatty acids and the fatty acid composition of lysoPC was accomplished by the procedures described by Ryals and Thompson (1987). Fatty acid methyl esters were made from the lipids by adding 5% HCl in methanol and heating for 2 h at 80°C in a sealed ampule. The fatty acid methyl esters were extracted in hexane and quantified by gas chromatography on a model 3700 gas chromatograph (Varian Associates, Inc., Palo Alto, CA).

Osmotic Shock and Radioisotope Labeling

Procedures for preparing cells, inducing hyperosmotic shock, and radiosotope labeling have been described previously (Einspahr et al., 1988). Hyperosmotic shock was induced by rapidly (2–4 s) adding an equal volume of 5.12 M NaCl-containing medium to cells in suspension. This raised the NaCl content to 3.43 M NaCl, or twice the normal NaCl content.

To prelabel cells, 300 μCi of $^{32}P_i$ was added to one culture, and the cells were grown for an additional 48 h. The cells were then centrifuged, and the pelleted cells were resuspended in phosphate-free growth medium. These cells were incubated for an additional 40 min before initiation of osmotic experiments. For experiments in which short-term $^{32}P_i$ incorporation into phospholipid was analyzed, 100 μCi of $^{32}P_i$ was added to 1×10^9 cells suspended in 20 ml of phosphate-free growth medium. After addition of label, cells were divided into two 10-ml portions, an experimental and a control. 2 min after addition of label, osmotic shock was initiated in the experimental portion, using phosphate-free 5.12 M NaCl-containing medium.

Results

Effects of Hyperosmotic Shock on Cell Structure

General Effects of Osmotic Stress on Cell Size. For the present studies *D. salina* was routinely grown in a medium containing 1.71 M NaCl. Rapid elevation of the NaCl concentration to 3.42 M caused a nearly instantaneous shrinkage of the cells from their typical oval shape to a cucumber-shaped prolate ellipsoid 1.20 times the length and 0.76 times the width of unstressed cells (Table I). Based on diameter measurements made from light micrographs, the average cells' volume was estimated to decrease during the first 3 min after hyperosmotic shock to 0.67 the control value, after which there was no further decrease. The cells gradually recovered in size and shape over a period of 16 h, by which time they had nearly regained their original size and shape.

Following the initial cell shrinkage, the surface of the cells was highly wrinkled (Fig. 1 *a*). Measurements made on enlarged thin section micrographs of these cells revealed that the surface area of the PM did not change as a result of the shock-induced volume decreae (Table I), although a number of intracellular organelles, including the N, Mt, Ch, Gol, and V decreased both in volume (Table II) and surface area (Table III). (Volume decreases in Ch and Gol were small and not statistically significant.) During the same period, the ER and Va increased their surface area (Table III).

Effects of Hyperosmotic Stress on Plasma Membrane (PM) Structure. Freeze-fracture replicas made of cells immediately after shrinkage (Fig. 1, *b* and *c*) and 60 min after shrinkage (Fig. 1, *d* and *e*) revealed a lower density of IMP on the PM E-face (Fig. 1 *c*) and P-face (Fig. 1 *d*), respectively. The latter exhibited many dome-shaped invaginations, the tops of which contained a lower density of IMP than were found in the surrounding PM (Fig. 1, *d* and *e*).

During the period after hyperosmotic shock, there was a significant decrease in the density of IMP, becoming apparent first on the E-face (within 3 min) and then on the P-face (within 60 min after shock) (Table IV). This change was unexpected in view of the fact that morphometric analysis indi-

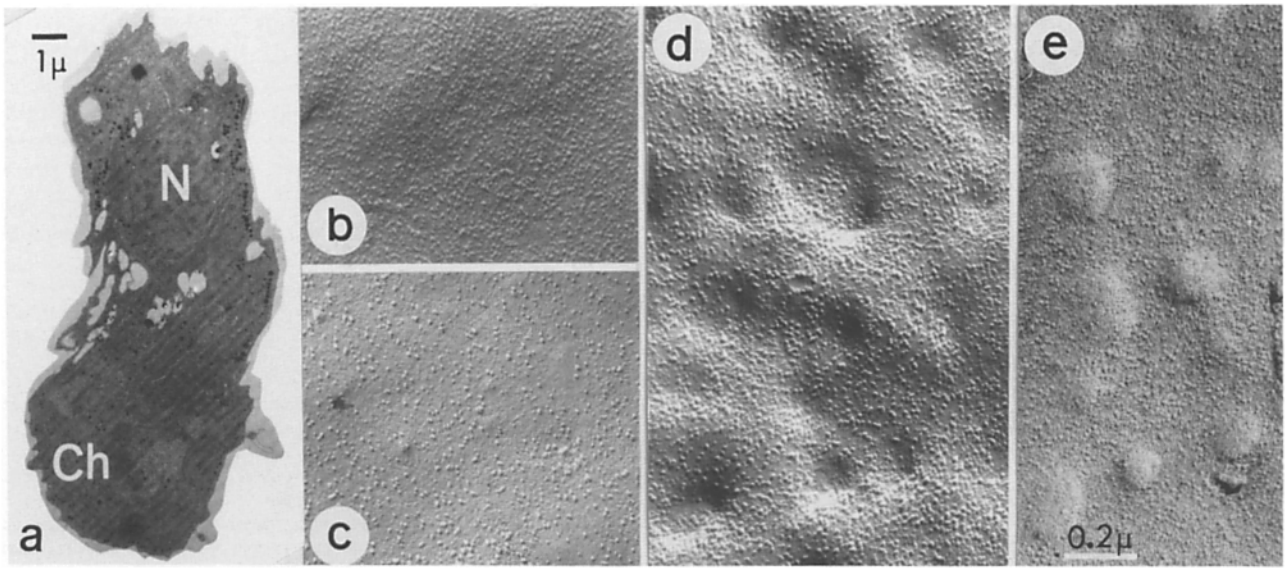

Figure 1. Dunaliella salina whole cell and PM after hyperosomotic shock. Culture medium osmolarity was rapidly raised from the normal 1.71–3.42 M NaCl, and cells were observed by (*a*) thin-section and (*b–e*) freeze-fracture electron microscopy. (*a*) Thin-section electron micrograph of a cell fixed 3 min after hyperosmotic shock, showing many irregularly concave shapes (invaginations) of PM. Larger vacuoles are seen in the cytoplasm. *Ch*, chloroplast; *N*, nucleus. (*b*) P-face of PM immediately (<5 s) after hyperosmotic shock. (*c*) E-face of PM immediately after hyperosmotic shock. It has a reduced number of IMP, but invaginated structures on PM are not clearly seen (cf. Fig. 1 *e*). (*d*) P-face of PM 60 min after hyperosmotic shock. Dome-shaped invaginations are seen on the PM. (*e*) Several convex dome-shaped structures are seen on the E-face of PM 60 min after the hyperosmotic shock. Bars: (*a*) 1 μm; (*b–e*) 0.2 μm.

Table II. Volume Changes in Major D. salina Cell Compartments after Hyperosmotic Shock

Cell compartment	Control culture		Stressed culture*		
	Volume	Volume	Volume	Volume	Vol stressed / Vol control
	μm^3/cell	% total	μm^3/cell	% total	
Chloroplast	301.3	51.5	229.3	57.6	0.76 NS
Nucleus	66.2	11.2	45.4	11.4	0.69
Vacuoles‡	27.8	4.7	29.3	7.4	1.05§
Mitochondria	16.0	2.7	6.0	1.5	0.38
Golgi bodies	2.3	0.4	2.0	0.5	0.87 NS
Lipid bodies	3.5	0.6	6.0	1.5	1.71‖
Cytoplasm	173.7	29.4	80.2	20.1	0.46
Total cell	590.8	100	398.2	100	

Volumes were determined by the morphometric procedures described in Materials and Methods. Except where noted, differences between values for stressed and control cultures were statistically significant at $P < 0.001$.
* Cells were fixed for analysis 3 min after increasing NaCl concentration from 1.71 to 3.42 M.
‡ Vacuoles sometimes contained small vesicles (≤0.25 μm diameter).
§ $P < 0.005$.
‖ $P < 0.2$.

Table III. Alterations in Organelle Surface Area Induced by Hyperosmotic Shock

Organelle	Surface area		Area stressed / Area control
	Control	Stressed*	
	m^2/cell	μm^2/cell	
Chloroplast	249.3	231.0	0.93
Nucleus	79.3	56.9	0.72
Mitochondria	87.4	48.6	0.56
Golgi bodies	32.9	31.2	0.95
Endoplasmic reticulum	697.1	775.3	1.11
Vesicles (≤0.25 μm)	115.2	85.2	0.74
Vacuoles (>0.25 μm)	94.5	126.5	1.34

Morphometric analysis of surface area utilized a minimum of 19 separate measurements for each value. The surface area/cell for each organelle was calculated as described in Materials and Methods. All differences between control and stressed cells are statistically significant at $P < 0.001$.
* Cells were fixed for analysis 3 min after increasing NaCl concentration from 1.71 to 3.42 M.

cated no decrease in PM surface area (Table I), and might reflect a coalescence of some IMP within the bilayer rather than a decrease in protein content.

Effects of Hyperosmotic Stress on the Chloroplast Envelope. Shrinkage of the cells frequently led to a separation of the outer membrane of the Ch envelope from the inner membrane (Fig. 2). A similar 'blistering' of the outer membrane (OE) has been observed in pea Ch subjected to hypertonic stress (Cline et al., 1985). Points of apparent fusion between the OE and elements of the ER were evident in the thin-section micrographs (Fig. 2 *b*). Freeze-fracture replicas revealed irregularly surfaced, elevated structures (Figs. 3 and 4) thought to correspond to these regions of distended OE. Here too the ER appeared to fuse with these structures (Fig. 4, *arrow*) and, in some cases, with Mt and the nuclear envelope (data not shown). The elevated regions of OE, which had an IMP density similar to that of the smooth regions (Table IV), were not present in replicas of cells fixed immediately after increasing the NaCl concentration.

Also prominent on the OE after hyperosmotic shock were patches of aggregated IMP (Fig. 3). Patches observed in cells exposed to high salt for 3 min had an IMP density equivalent to ~2,000 particles/μm^2, although the actual size of each patch was quite small, averaging 16 IMP/patch. By 60 min after hyperosmotic shock, the average patch size had increased to 170 IMP/patch, but the number of patches per Ch had decreased as would be expected (assuming the observed replicas were representative) if the total number of particles per Ch had been maintained.

The presence of aggregated IMP patches in OE of hyperosmotically stressed cells was reminiscent of particle aggregations resulting from low temperature–induced lipid phase separations (Kitajima and Thompson, 1977). However, *Dunaliella* cells first shocked by exposure to high salt for 3 min and then suddenly chilled to 2°C before fixation for freeze-fracture EM exhibited a distribution of IMP similar to that found in unchilled cells. If the salt-induced patches had formed as the result of a lipid phase separation, chilling should have complemented the effect and promoted even more extensive aggregations. IMP aggregation in this case is more likely to stem from an effect of salt upon the membrane proteins themselves. Thus while additional IMP aggregation

Table IV. Change in Density of Intramembranous Particles (IMP) in the Plasma Membrane and Outer Membrane of the Chloroplast Envelope after Hyperosmotic Shock

Membrane	Fracture face	Control cells	Time (after shock) of cell fixation		
			0 min	3 min	60 min
Plasma membrane	P-F	3508 ± 548 (13)	3372 ± 665 (25)	2533 ± 540* (10)	2740 ± 453* (27)
	E-F	2085 ± 301 (10)	1191 ± 322* (32)	1911 ± 463 (19)	1875 ± 196‡ (13)
Outer membrane of chloroplast envelope	P-F	1172 ± 434 (19)	1365 ± 559 (34)	1228 ± 422 (29)	1264 ± 456 (25)
	E-F	893 ± 429 (34)	711 ± 460‡ (45)	823 ± 584 (26)	889 ± 632 (36)

Values are mean (IMP/μm^2) ± SD. Numbers of areas counted (from several representative cells) are shown in parenthesis.
* Difference from control value is statistically significant at $P < 0.001$.
‡ Difference from control value is statistically significant at $P < 0.1$.

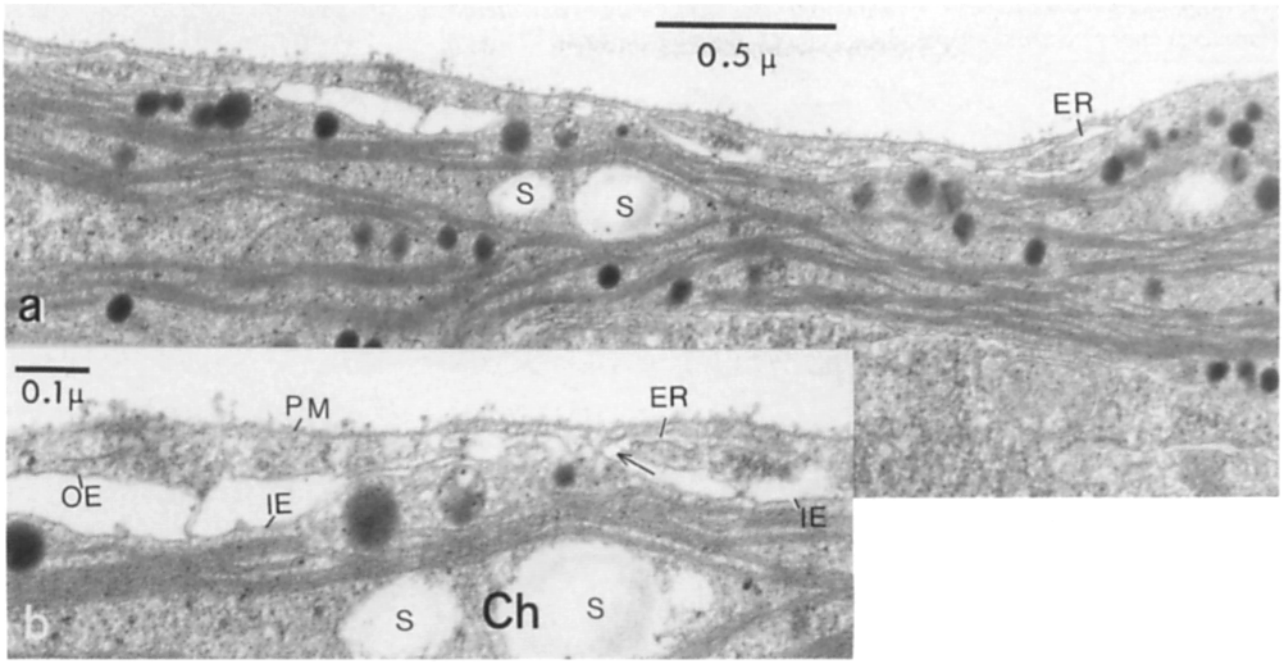

Figure 2. Thin-section micrograph of cell 3 min after hyperosmotic shock. The outer membrane of the Ch envelope (*OE*) is separated from the inner membrane (*IE*), forming elevated structures as shown in Fig. 3. Some of these elevated structures are connected to ER (Fig. 4 *b*, *arrow*). *S*, starch grain. Bars: (*a*) 0.5 μm; (*b*) 0.1 μm.

could not be effected by low temperature, it was induced when cells were stressed by exposure to an even higher (4.28 M) concentration of NaCl (data not shown).

Effect of Hyperosmotic Stress on Other Membranous Organelles. Whereas all major cellular compartments either maintained a constant volume or decreased in volume after hyperosmotic shock (Tables I and II), certain types of membrane, most notably the ER, actually increased in surface area. Based upon the ultrastructural indications of fusion observed in these studies together with similar evidence obtained with hypoosmotically shocked *Dunaliella* (Maeda and Thompson, 1986), we propose that the ER serves as a reservoir for membrane material present in temporary excess during the initial hyperosmotic stress period when the Ch and certain other organelles shrink. A balance sheet of these changes (Table V) indicates that the increase in the ER surface area can accommodate the losses sustained by these organelles. Not included in these calculations are the small (≤0.25 μm diameter) vesicles and the larger (>0.25 μm diameter) vacuoles which seem to lack the specificity for fusing with ER, Mt, and Ch (Maeda and Thompson, 1986).

Effects of Hyperosmotic Shock on Phospholipid Metabolism

In view of the dramatic decline in polyphosphoinositide content triggered by hypoosmotic shock (Einspahr et al., 1988), changes in lipid metabolism were also monitored after the hyperosmotic shock just described. A limited study measuring changes in the amounts of certain individual phospholipid classes in *D. salina* cells labeled with $^{32}P_i$ to isotopic equilibrium (Einspahr et al., 1988) had already indicated a very different behavior. Suddenly raising the NaCl concentration from 1.71 to 3.42 M caused a 30% elevation rather than a fall in the mass of cellular PIP_2 (Fig. 5 *a*). The amount of PA in the cell also responded to hyperosmotic shock quite differently, plunging within 2 min to <60% of control values (Fig. 5 *a*) in contrast to the 40% rise under hypoosmotic conditions (Einspahr et al., 1988).

Additional experiments utilizing ^{32}P-labeling to isotopic equilibrium confirmed the above findings and showed that the phospholipids of major importance in quantitative terms, namely phosphatidylcholine (PC), phosphatidylglycerol (PG), and phosphatidylethanolamine (PE), experienced little change in amount when cells were exposed to high salt (Fig. 5 *b*). However, careful analysis of the minor lipid com-

Table V. Hyperosmotic Stress-induced Changes in Surface Areas of Organelle Classes Interacting by Apparent Fusion

	Increase (μm²)*		Decrease (μm²)*	
	Vacuoles	32.0	Vesicles	30.0
			Golgi bodies	1.7
Subtotal		32.0		31.7
	Endoplasmic reticulum	78.2	Chloroplast	18.3
			Nucleus	22.3
			Mitochondria	38.8
Subtotal		78.2		79.4
Total		110.2		111.1

* Changes, in μm², measured 3 min after increasing NaCl concentration from 1.71 to 3.42 M.

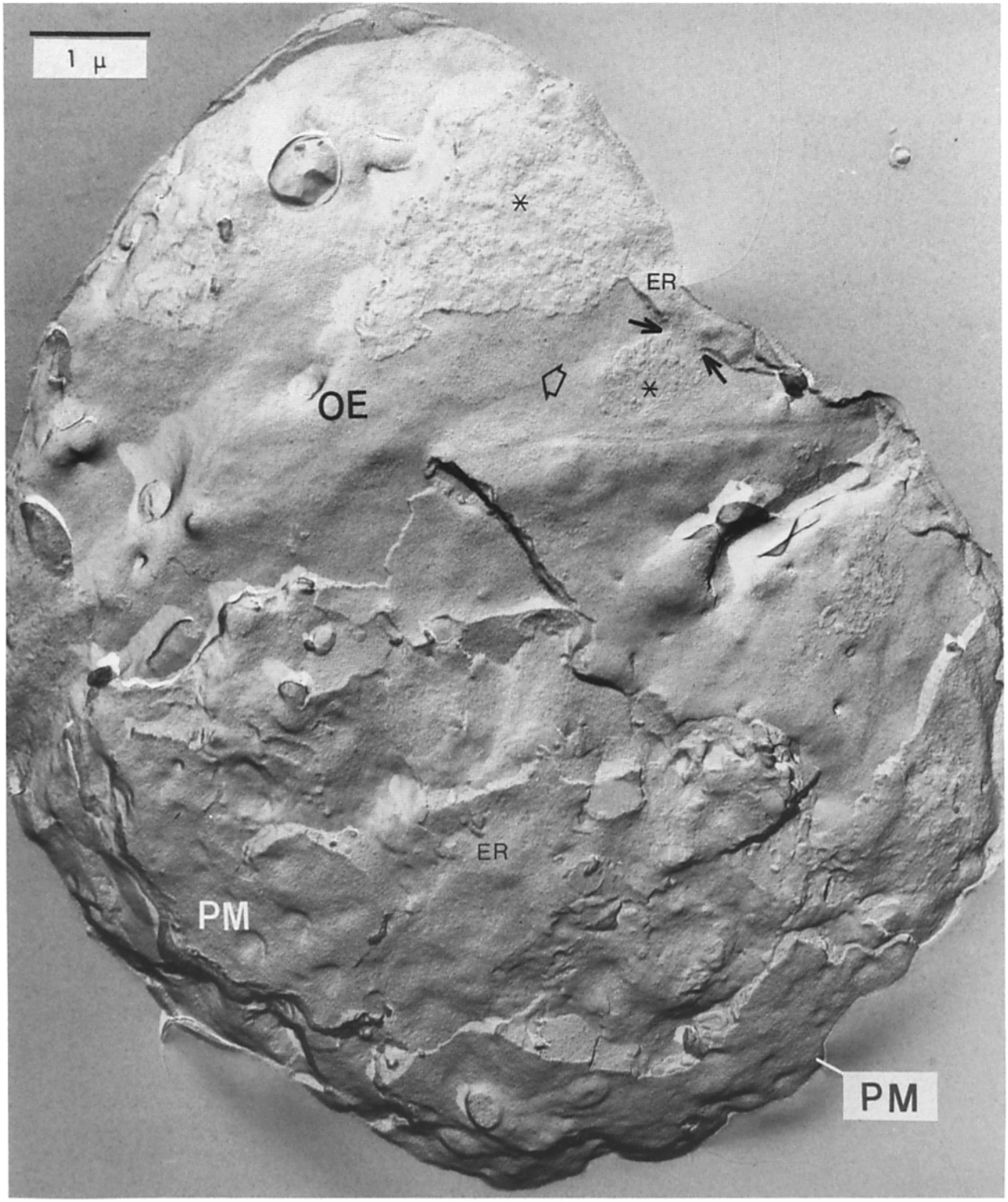

Figure 3. Freeze-fracture electron micrograph of a cell fixed 60 min after hyperosmotic shock. ER occupies large areas between the PM and outer membrane of the Ch envelope (*OE*). Three irregular flat elevations (*) are seen on the OE, showing continuity to ER membrane (*arrows*). On the OE, intramembranous aggregation patches (*wide arrow*) are seen. Bar, 1.0 μm.

ponents detected a marked elevation in lysoPC, which rose within 10 min after the hyperosmotic shock to a level >200% of controls (Fig. 5 *b*), and lysoPA, which increased to nearly 400% of control values during the same period (Fig. 5 *a*). Lysophosphatidylinositol and lysophosphatidylethanolamine did not increase (data not shown).

Despite the large relative increases in mass sustained by lysoPC and lysoPA in the hyperosmotically stressed cells,

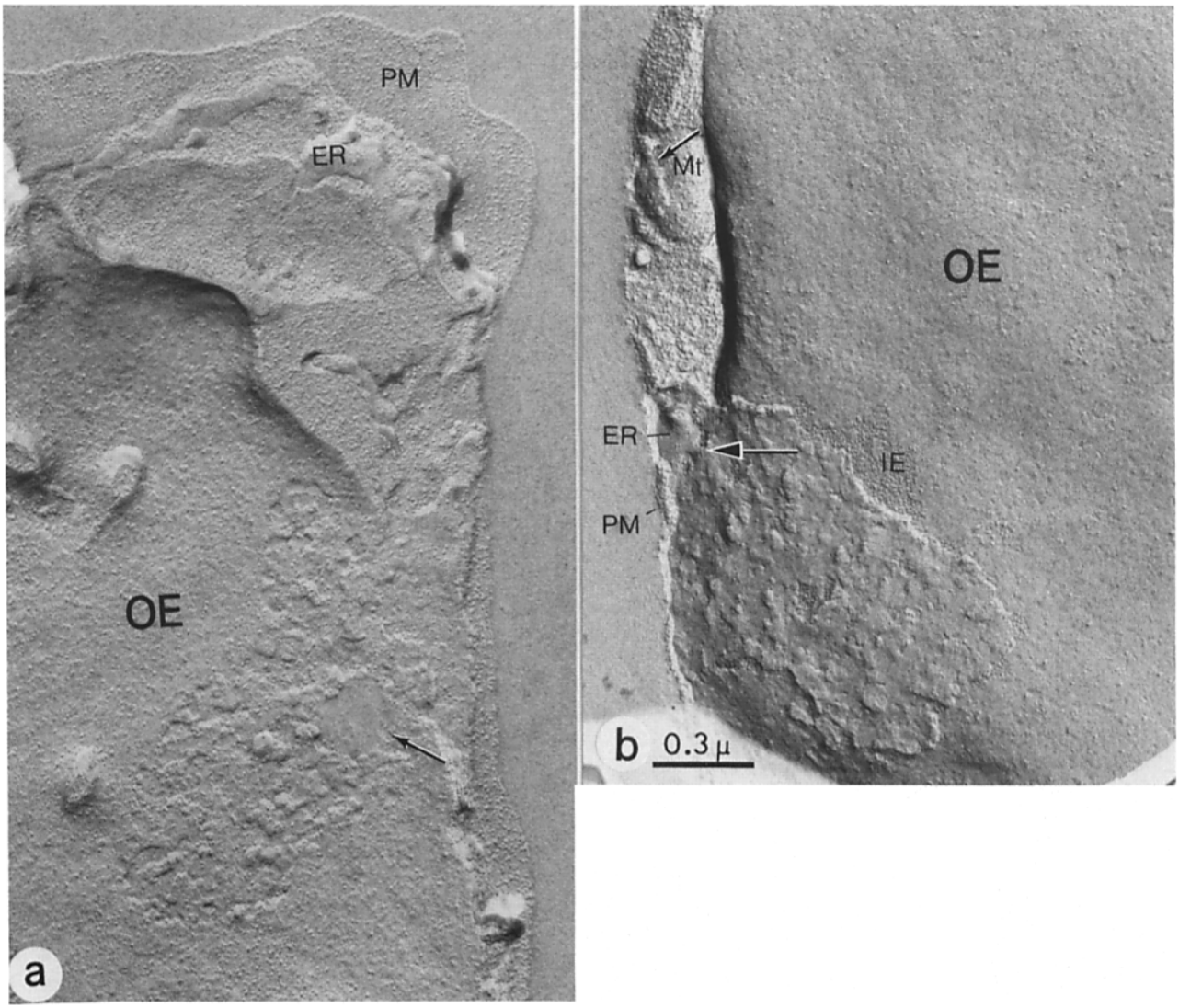

Figure 4. Freeze-fracture electron micrographs of the outer membrane of a Ch envelope (*OE*) fixed 60 min after hyperosmotic shock. (*a*) P-face of OE with flat depression showing continuity to ER membrane (*arrow*). (*b*) E-face of OE with flat elevation continuous with the ER membrane (*larger arrow*). Around the elevation, a small area of inner Ch envelope (*IE*) is seen (*b*). Bar, 0.3 μm. On the Mt, a similar elevation appears (*smaller arrow*).

these two lipids together still accounted for <2.0 mol% of the total cellular phospholipids as compared with their combined resting levels of <0.6 mol%. But their key position as intermediates in phospholipid metabolism prompted us to assess their involvement further through the use of pulse-labeling experiments. Cells resuspended in phosphate-free medium were treated with $^{32}P_i$ and then, after 2 min, one half of the suspension was exposed to hyperosmotic conditions. Analysis of individual lipid classes after increasing periods of stress revealed that ^{32}P incorporation into PG and PE was slightly depressed (Fig. 6, *a* and *b*), whereas the labeling of PC and lysoPC was much higher in stressed cells than in controls (Fig. 6, *c* and *d*). Further experiments utilizing ^{32}P pulse labeling indicated changes in ^{32}P incorporation into PA and PIP_2 (Fig. 7). These changes coincided with the alterations in mass observed for these phospholipids (Fig. 5 *a*). Although no appreciable change was detected in the mass of PI, pulse-labeling experiments indicated that at later time points from 10 to 30 min after hyperosmotic shock, the rate of ^{32}P incorporation into this phospholipid slowed, indicating a change in metabolism of PI (Fig. 7).

The lysoPC labeling differential was most striking, with stressed cells containing fivefold the amount of radioactivity as control cells after 10 min (Fig. 6, *c* and *d*). The much larger PC pool sustained a 2.5-fold enhancement in labeling with respect to nonstressed cells, despite the fact that the amount of PC remained constant. This indicates a stimulation of metabolic turnover. Additional characterization of the lysoPC pool was achieved through gas chromatographic analysis of the component fatty acids. LysoPC isolated subsequent to hypoosmotic shock contained almost exclusively one of two saturated fatty acids, palmitic and stearic acids, with palmitic being the predominant species. Because these fatty acids are characteristically found at the *sn*-1 position of

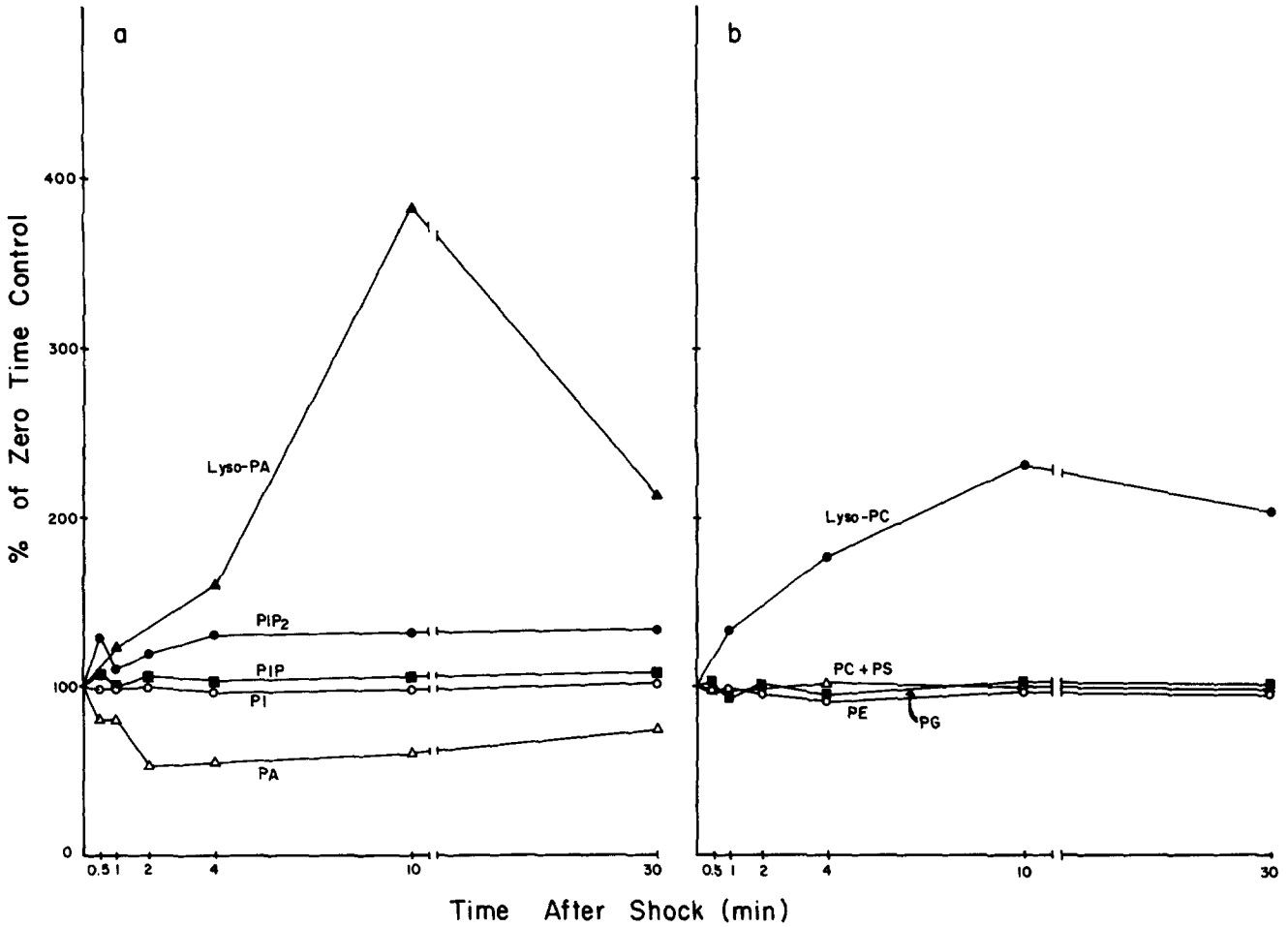

Figure 5. Hyperosmotic shock-induced changes in the mass of ^{32}P-prelabeled phospholipids. One cell culture was prelabeled for at least 48 h with 300 μCi of $^{32}P_i$. Cells were harvested and resuspended in 10.5 ml of phosphate-free growth medium. Hyperosmotic shock was induced by the addition of an equal volume of growth medium containing 5.12 M NaCl, raising the final NaCl content to twice the normal level. Aliquots containing 1×10^8 cells were taken at the indicated time points. Two control samples were taken before osmotic shock. Results are the mean from four to five independent experiments. Values are expressed as percent of nonstressed control values.

PC in *D. salina* (Lynch and Thompson, 1984 *a*, *b*), the lysoPC formed consequent to hyperosmotic shock is clearly 1-acylglycerophosphorylcholine.

Because of the elevation observed in the mass of certain lysophospholipids, the free fatty acid pool was analyzed for a potential elevation which might correlate with the changes seen for lysophospholipids after hyperosmotic shock. The results of such an analysis revealed that the total fatty acid pool increased to 124% of control 10 min after hyperosmotic shock. This increase was due primarily to elevations in the level of linolenic acid (58% increase) and palmitic acid (15% increase).

Discussion

Dunaliella possesses the capacity to alter its internal osmolarity very rapidly in response to changing external NaCl levels. One extensively studied mechanism for restoring isotonic balance involves increasing or decreasing the internal glycerol concentration in response to hyper- or hypoosmotic stress, respectively (Brown and Borowitzka, 1979; Peeler, T., and G. Thompson, unpublished observations). To augment the relatively slow (1 h to completion) changes in the absolute amount of glycerol, an almost instantaneous change in osmolarity can be effected by stress-induced alterations in cell volume. We have recently described the extent and the mechanisms by which key *D. salina* membranes expand during hypoosmotic stress (Maeda and Thompson, 1986). When *D. salina* is quickly diluted from a 1.71 M NaCl medium to one containing 0.85 M NaCl, an immediate uptake of water causes the surface area of its PM to expand within seconds by a factor of 1.56. This is achieved through fusion with the PM of a population of small vesicles normally located nearby in the cytoplasm. However, the reverse stress described in the present communication, namely, the sudden exposure of cells grown in 1.71–3.42 M NaCl, did not deplete the PM surface area by reversing the fusion phenomenon. On the contrary, the sizeable decrease in cell volume (Table I) was accompanied by a general infolding of the PM (Fig. 1 *a*) without apparent loss of material from the membrane (Table I).

The failure of the plasma membrane to undergo endocytotic vesiculation during cell shrinkage was rather unexpected because such a mechanism of surface area reduction has been clearly indicated in dehydrating rye protoplasts (Gordon-Kamm and Steponkus, 1984 *a* and *b*). The response in *D. salina* was perhaps more akin to that of cell wall-enclosed rye cells, in which contraction was associated

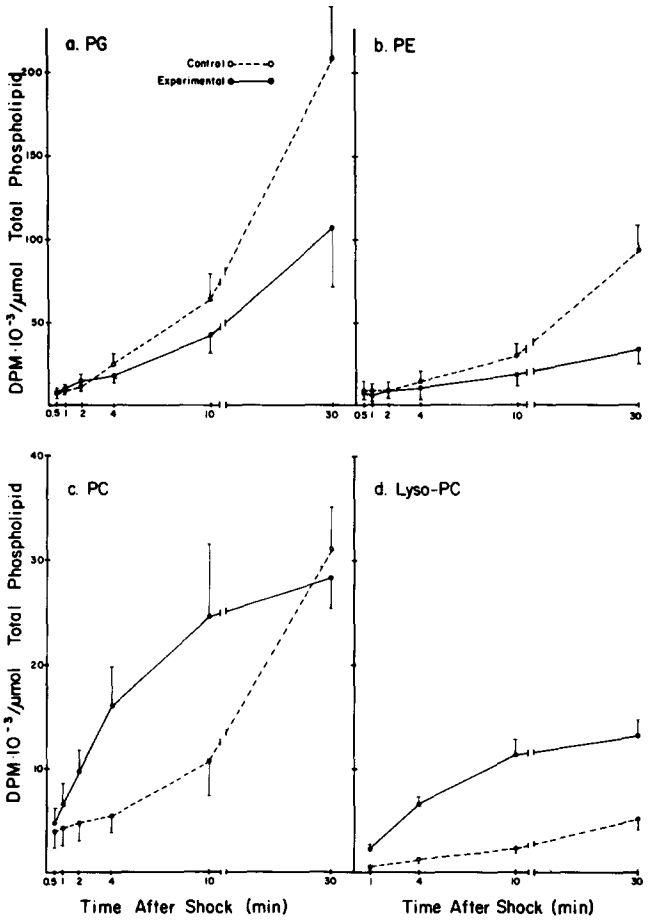

Figure 6. Time course of hyperosmotic shock-induced alterations in $^{32}P_i$ incorporation into *D. salina* major phospholipids and lysoPC. 100 μCi of $^{32}P_i$ were added to 20 ml of a cell suspension containing 1×10^9 cells in phosphate-free growth medium. Cells were divided into two 10-ml portions, an experimental and a control. Hyperosmotic shock (●) was initiated 2 min after addition of $^{32}P_i$ by adding 10-ml of growth medium (phosphate-free) containing 5.12 M NaCl, raising the final NaCl content to twice the normal level. To the control portion (○) was added 10 ml of normal growth medium (phosphate-free). Aliquots were taken at the indicated time points and processed as described in Materials and Methods. Results are the mean ± SE from three independent experiments.

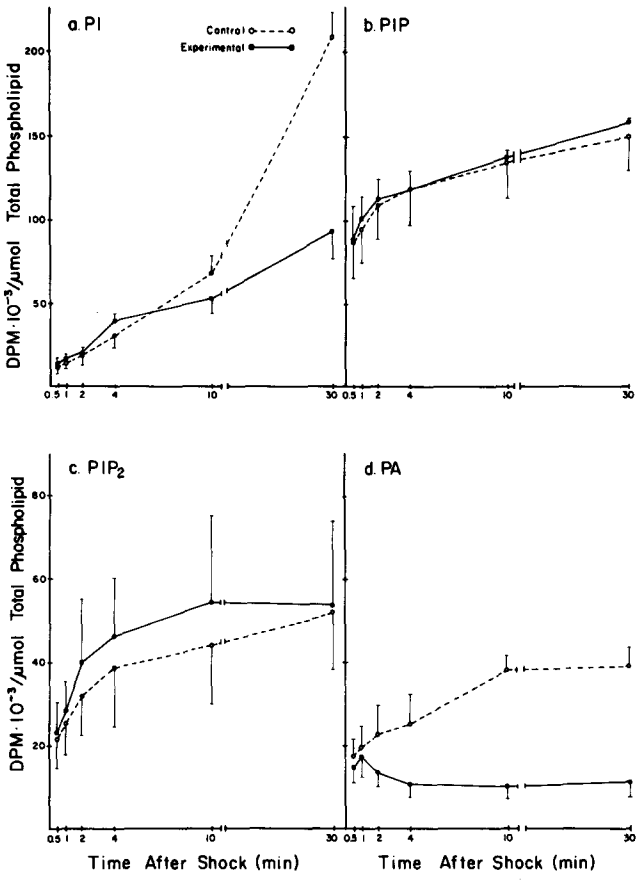

Figure 7. Time course of hyperosmotic shock-induced alterations in $^{32}P_i$ incorporation into *D. salina* inositol phospholipids and PA. The procedures followed were identical to those outlined in Fig. 6. Results are the mean ± SE from three independent experiments.

with PM intrusions into the cytoplasm and with cell wall–attached tubular extensions of the PM (Johnson-Flanagan and Singh, 1985). As the cell volume decreased, both types of membrane extensions remained joined to the PM, effectively conserving its surface area.

In contrast to the PM, the principal *D. salina* intracellular organelles (N, Mt, Ch) changed their surface areas as well as volumes during hyperosmotically induced cell shrinkage (Tables II and III). Evidence from thin-section electron micrographs (Figs. 2–4) and from morphometric analysis (Table III) indicates that these organelles transferred some of their surface membrane via a fusion process to elements of ER during volume loss. A balance sheet shows that the increase in ER surface area during a 3-min period after hyperosmotic shock almost exactly equalled the decrease in surface area of these organelles (Table V). This response is precisely the opposite response to that observed for these organelles during cell expansion triggered by dilution of the external salt concentration (Maeda and Thompson, 1986).

The alterations in lipid metabolism induced by hyperosmotic shock were as fundamentally different from those caused by hypoosmotic shock as were the patterns of ultrastructural changes induced by the two types of osmotic shock. The rise in polyphosphoinositides and the fall in PA after hyperosmotic shock (Fig. 5 *a*) were opposite to the response induced by hypoosmotic conditions (Einspahr et al., 1988). Hyperosmotic conditions stimulated the metabolic turnover of PC and led to an accumulation of its intermediate, lysoPC, in significant amounts. These changes were not seen after hypoosmotic shock.

The precise relationships between the observed ultrastructural rearrangements and changes in phospholipid metabolism are not clear. However, the various intracellular organelles of *D. salina* are each likely to maintain a distinct phospholipid composition which serves a functionally defined purpose distinct for that organelle. Thus the changes in phospholipid metabolism may be one mechanism to retailor membrane components incorporated into the ER from various other organelles upon hyperosmotic shock. In such a way the ER may maintain or recover its distinctive lipid composition. This may, in part, explain the increase in PC turnover without an apparent loss of mass. The ER (main component of microsomes obtained by *D. salina* cell fractionation) is the membrane most highly enriched (32% of total lipid phosphorus) in PC (Lynch and Thompson, 1984 *a*, *b*; Peeler, T., and K. J. Einspahr, manuscript in preparation), while the fraction lowest in PC, at 17% of total lipid phos-

phorus, is the PM. If one or more of the membranes contributing, through fusion, to the 1.5-fold increase in ER after hyperosmotic shock is also relatively low in PC, supplementary PC biosynthesis and retailoring may be necessary to restore a lipid composition typical of ER in this expanded fraction.

In addition to the increased de novo PC synthesis suggested by the ^{32}P labeling data, the rise in lysoPC and free fatty acids indicates an increased phospholipase A activity. Indeed, the increase in PC formation could be secondary to the phospholipase A hydrolysis of PC, because an elevated level of free fatty acids is known to initiate the translocation of CTP/phosphocholine cytidylyl transferase from cytosol to membranes (Cornell and Vance, 1987; Weinhold et al., 1984), activating it in the process (Anderson et al., 1985; Pelech et al., 1983). Unsaturated fatty acids appear to be particularly effective in stimulating this process (Whitlon et al., 1985; Pelech et al., 1984). Interestingly, a phenomenon very similar to the concomitant stimulation of PC synthesis and breakdown with little change in absolute mass which we report in this investigation has also been reported by Kent (1979). When phospholipase C was added to the culture medium of embryonic chick muscle cells, a fivefold increase of ^{32}P incorporation into PC occurred that was paralleled by a similar increase in the rate of PC breakdown. The increased rate of PC synthesis was sufficient to prevent an overall loss of PC content.

There are precedents for an increased phospholipase A activity under hyperosmotic conditions. A selective stimulation of phospholipid fatty acid turnover involving an apparent simultaneous stimulation of a phospholipase A and acyltransferase acting primarily on phosphatidylethanolamine has been reported for erythrocytes exposed to hypertonic medium (Dise et al., 1980). In addition, hyperosmotic stress in vitro has been shown to activate phospholipase A_2 associated with liposomes (Okimasu et al., 1984). Based on in vitro studies of phospholipase A_2, Romero et al. (1987) and Menashe et al. (1986) have suggested that structural alterations in the lipid bilayer surface may be the key factor in triggering activation of the enzyme. Such alterations might be likely to occur under conditions of hypertonic shock when the cell volume rapidly decreases and membrane physical properties might also change rapidly.

We are grateful to the Cell Research Institute, University of Texas, for the use of their electron microscopy facilities, and to Dr. P. E. Ryals and Dr. T. C. Peeler for constructive comments during manuscript preparation.

This work was supported in part by grants from the National Science Foundation (DMB 8506750), the Robert A. Welch Foundation (F-350), the National Cancer Institute (IT32CA09182), and the Texas Advanced Technology Research Program.

Received for publication 22 February 1988, and in revised form 11 April 1988.

References

Anderson, K. E., D. S. Whitlon, and G. C. Mueller. 1985. Role of fatty acids in the reversible activation of phosphatidylcholine synthesis in lymphocytes. *Biochim. Biophys. Acta.* 835:360–368.

Bartlett, G. R. 1959. Phosphorus assay in column chromatography. *J. Biol. Chem.* 234:466–468.

Brown, A. D., and L. J. Borowitzka. 1979. Halotolerance of *Dunaliella*. *In* Biochemistry and Physiology of Protozoa. Vol. 1. Second ed. M. Levandowsky and S. H. Hunter, editors. Academic Press, New York. 139–190.

Cline, K., K. Keegstra, and L. A. Staehelin. 1985. Freeze-fracture electron microscopic analysis of ultrarapidly frozen envelope membranes on intact chloroplasts after purification. *Protoplasma.* 123:83–94.

Cornell, R., and D. E. Vance. 1987. Translocation of CTP:phosphocholine cytidylyltransferase from cytosol to membranes in HeLa cells: stimulation by fatty acid, fatty alcohol, mono- and diacylglycerol. *Biochim. Biophys. Acta.* 919:32–36.

Dise, C., D. B. P. Goodman, and H. Rasmussen. 1980. Selective stimulation of erythrocyte membrane phospholipid fatty acid turnover with decreased cell volume. *J. Biol. Chem.* 255:5201–5207.

Einspahr, K. J., T. C. Peeler, and G. A. Thompson, Jr. 1988. Rapid changes in polyphosphoinositide metabolism associated with the response of *Dunaliella salina* to hypoosmotic shock. *J. Biol. Chem.* 263:5775–5779.

Gordon-Kamm, W. J., and P. L. Steponkus. 1984*a*. The behavior of the plasma membrane following osmotic concentration of isolated protoplasts: implications in freeze injury. *Protoplasma.* 123:83–94.

Gordon-Kamm, W. J., and P. L. Steponkus. 1984*b*. Lamellar-to-hexagonal II phase transitions in the plasma membrane of isolated protoplasts after freeze-induced dehydration. *Proc. Natl. Acad. Sci. USA.* 81:6373–6377.

Johnson-Flanagan, A. M., and J. Singh. 1985. Plasma membrane deletion during plasmolysis in isolated rye cells. *Plant Physiol.* (Bethesda). 77:15. (Abstr.)

Jolles, J., K. W. A. Wirtz, P. Schotman, and W. H. Gispen. 1979. Pituitary hormones influence polyphosphoinositide metabolism in rat brain. *FEBS (Fed. Eur. Biochem. Soc.) Lett.* 105:110–114.

Kent, C. 1979. Stimulation of phospholipid metabolism in embryonic muscle cells treated with phospholipase C. *Proc. Natl. Acad. Sci. USA.* 76:4474–4478.

Kitajima, Y., and G. A. Thompson, Jr. 1977. *Tetrahymena* strives to maintain the fluidity of all its membranes constant. Electron microscope evidence. *J. Cell Biol.* 72:744–755.

Lynch, D. V., and G. A. Thompson, Jr. 1982. Low temperature-induced alterations in the chloroplast and microsomal membranes of *Dunaliella salina*. *Plant Physiol. (Bethesda).* 69:1369–1375.

Lynch, D. V., and G. A. Thompson, Jr. 1984*a*. Microsomal phospholipid molecular species alterations during low temperature acclimation in *Dunaliella*. *Plant Physiol. (Bethesda).* 74:193–197.

Lynch, D. V., and G. A. Thompson, Jr. 1984*b*. Chloroplast phospholipid molecular species alterations during low temperature acclimation in *Dunaliella*. *Plant Physiol. (Bethesda).* 74:198–203.

Maeda, M., and G. A. Thompson, Jr. 1986. On the mechanism of rapid plasma membrane and chloroplast expansion in *Dunaliella salina* exposed to hypoosmotic shock. *J. Cell Biol.* 102:289–297.

Marinetti, G. V. 1962. Chromatographic separation, identification, and analysis of phosphatides. *J. Lipid Res.* 3:1–11.

Menashe, M., G. Romero, and R. L. Biltonen. 1986. Hydrolysis of dipalmitoylphosphatidylcholine small unilamellar vesicles by porcine pancreatic phospholipase A_2. *J. Biol. Chem.* 261:5328–5333.

Okimasu, E., J. Sasaki, and K. Utsumi. 1984. Stimulation of phospholipase A_2 activity by high osmotic pressure on cholesterol-containing phospholipid vesicles. *FEBS (Fed. Eur. Biochem. Soc.) Lett.* 168:43–48.

Pelech, S. L., P. H. Pritchard, D. N. Brindley, and D. E. Vance. 1983. Fatty acids promote translocation of CTP:phosphocholine cytidylyltransferase to the endoplasmic reticulum and stimulates rat hepatic phosphatidylcholine synthesis. *J. Biol. Chem.* 258:6782–6788.

Pelech, S. L., H. W. Cook, H. B. Paddon, and D. E. Vance. 1984. Membrane bound CTP:phosphocholine cytidylyltransferase regulates the rate of phosphatidylcholine synthesis in HeLa cells treated with unsaturated fatty acids. *Biochim. Biophys. Acta.* 795:433–440.

Romero, G., K. Thompson, and R. L. Biltonen. 1987. The activation of porcine pancreatic phospholipase A_2 by dipalmitoylphosphatidylcholine large unilamellar vesicles. *J. Biol. Chem.* 262:13476–13482.

Rouser, G., S. Fleischer, and Y. Yamamoto. 1970. Two dimensional thin layer chromatographic separation of polar lipids and determination of phospholipids by phosphorous analysis of spots. *Lipids.* 5:494–498.

Ryals, P. E., and G. A. Thompson, Jr. 1987. Alterations of the free fatty acid pool of *Tetrahymena* responding to low-temperature stress. *Biochim. Biophys. Acta.* 919:122–131.

Sekar, M. C., and L. E. Hokin. 1986. The role of phosphoinositides in signal transduction. *J. Membr. Biol.* 98:193–210.

Spurr, A. J. 1969. A low viscosity epoxy-rsin embedding medium for electron microscopy. *J. Ultrastruct. Res.* 26:31–43.

Toth, R. 1982. An introduction to morphometric cytology and its application to botanical research. *Am. J. Bot.* 69:1694–1706.

Weibel, E. R. 1979. Practical methods for biological morphometry. *In* Stereological Methods. Vol. 1. Academic Press, New York. 415.

Weinhold, P. A., M. E. Rounsifer, S. E. Williams, P. G. Brubaker, and D. A. Feldman. 1984. CTP phosphorylcholine cytidylyltransferase in rat lung. The effect of free fatty acids on the translocation of activity between microsomes and cytosol. *J. Biol. Chem.* 259:10315–10321.

Whitlon, D. S., K. E. Anderson, and G. C. Mueller. 1985. Analysis of the effects of fatty acids and related compounds on the synthesis of phosphatidylcholine in lymphocytes. *Biochim. Biophys. Acta.* 835:369–377.